A Compact High-Performance Patch Antenna Array for 60-GHz Applications

Wanlan Yang, Kaixue Ma, Senior Member, IEEE, Kiat Seng Yeo, Senior Member, IEEE, and Wei Meng Lim

***Abstract*—In this letter, a compact and high-performance patch antenna array is developed for 60-GHz applications. The method to enhance both the gain and the frequency bandwidth of the antenna array simultaneously by using a parallel-series feed network together with the differential feeding technique is studied thoroughly. The tested antenna array achieves operation bandwidth ($|S_{11}|$ < -10 dB) from 55 to 68 GHz, which covers worldwide 60-GHz unlicensed band of 57-66 GHz, with peak gain of 12.8-15.6 dBi. The measured -3 dB beamwidths at 61.5 GHz are around ±13° in E-plane and ±15° in H-plane respectively. The designed high gain antenna array has a compact size of only 20 mm × 14 mm excluding the connector footprint for test.**

***Index Terms*—60-GHz band, antenna array, parallel-series feed network, patch antenna, differential drive**

I. Introduction

In recent years, due to the demand of high data rate short range wireless communication, the worldwide unlicensed spectrum at 60-GHz band has attracted much attention. As one of the key components in 60-GHz wireless communication systems, the antenna need to be low cost, high performance, compact size and easily integrated with front-end circuitry for commercial applications. A few methods were investigated to suppress the surface wave loss for enhancing the antenna gain, such as a cavity inside the substrate [1]-[3], a soft-surface technique [4] and a uniplanar-compact electromagnetic band-gap (UC-EBG) structure on the substrate [5]. In addition, a grid antenna array and a vertical off-center-fed dipole antenna array on LTCC substrates were also reported in [6] and [7] with acceptable performances respectively, both of which were designed using multilayer LTCC technology through vertically connection vias. In general, LTCC technology can be used to improve antenna performance but the manufacturing cost would be high. In [8], by using a multilayer printed circuit boards (PCB) structure, a 60-GHz aperture-coupled dense dielectric (DD) patch antenna array was designed to achieve a gain up to 16.5 dBi and an impedance bandwidth of 23.7% from 51.3 to 65.1 GHz for $|S_{11}|$ < -10 dB, but with a large size of the antenna and the costly mechanical manufacturing. Compared to LTCC or multilayer PCB structures, the double sided PCB is lower in material cost and easier in fabrication. A substrate integrated waveguide (SIW) slot antenna array and a SIW cavity-backed slot antenna with high directional radiation but narrow impedance bandwidths of 4.1% and 6.5% were reported in [9] and [10] respectively. A parallel-series feed network was proposed for high radiation efficiency and reduced conductor traces in [11] by reducing the feed transmission line length and the number of curved transmission lines in the feed structure. Two different patch antenna arrays in [12] and a series-fed antenna array with a differential feeding technique in [13] exhibited the large size and the operation frequency ranges of only 59-61 GHz and 59-67 GHz respectively, which doesn't fully cover 9 GHz band of worldwide 60-GHz unlicensed band.

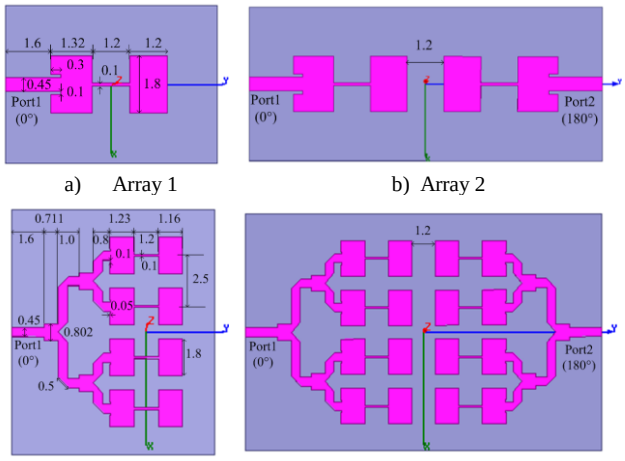

a) Array 1 b) Array 2

c) Array 3 d) Array 4

Fig. 1 Geometry of Array 1, Array 2, Array 3 and Array 4 (all dimensions are expressed in millimeters).

In this paper, to make antenna array fully cover the international 9 GHz bandwidth of 60-GHz band under the constraints of low cost, compact size and high gain, a method to enhance the gain and frequency bandwidth of the antenna array simultaneously by hybrid using a parallel-series feed network together with the differential feeding technique is studied thoroughly. The experimental results are well agreed with those of the simulation. The designed compact antenna array on a low cost single substrate PCB demonstrates a high radiation gain up to 15.6 dBi and broad bandwidth of 55-68 GHz fully covering the worldwide 60-GHz band from 57 to 66 GHz for IEEE802.11ad applications.

II. THE ANTENNA ARRAY DESIGN WITH PARALLEL-SERIES FEED NETWORK

The antenna array was designed and implemented on a Rogers RO4003C substrate with thickness of 0.203 mm, relative permittivity of 3.38 and loss tangent of 0.0027. Two copper layers are on the opposite sides of the substrate with conductivity $\sigma = 5.8 \times 10^7$ S/m and the thickness of the metal layers is 17 μm. The rectangular patch is used as the fundamental radiation element to take its advantages of low profile and planar structure. The bottom copper layer is used as the ground plane and the antenna elements with feed network are patterned on the top copper layer.

The geometries of the antenna arrays of four contrast cases i.e. Array 1, 2, 3 and 4 are shown in Fig. 1. The inputs of all antenna arrays are designed and optimized to 50-ohm. The simulated reflection coefficients and peak gains of four types of antenna arrays are compared in Fig. 2 while their simulated radiation patterns are in contrast in Fig. 3.

For Array 1 as shown in Fig. 1 a), a two-element series-fed patch antenna array with an inset feed is used. The width and depth of the two symmetrical rectangular notches can be tuned for impedance matching. As seen in Fig. 2 and Fig. 3(a), Array 1 shows a peak gain of 9.77 dBi at 61.9 GHz, a narrow impedance bandwidth of 60.0–62.4 GHz for $|S_{11}| < -10$ dB , an asymmetrical co-polarized radiation pattern in the E-plane and a high cross-polarization level in the H-plane.

Array 2 as shown in Fig. 1 b) is introduced by putting two identical sub-arrays in opposite with the two feeding point located symmetrically about X-axis. The two sub-arrays of the Array 2 have exactly the same dimensions as those of Array 1. The space between two sub-arrays has been optimized by HFSS simulation with optimum value of 1.2 mm. As observed from the simulated results in Fig. 2 and Fig. 3(b), Array 2 exhibits symmetrical co-polarized radiation patterns and low cross-polarization levels in both E- and H-plane with the peak gain of 12.32 dBi at 62.2 GHz when the port1 and port2 are excited with differential drive signals i.e. 180º out-of-phase signals in the same amplitude, but the impedance bandwidth of Array 2 is as narrow as that of Array 1.

As shown in Fig. 1 c), Array 3 connects four identical two-element series-fed sub-arrays in parallel by a one-to-four parallel-feed network. The design of the parallel-feed network is based on the quarter-wave matched T-junction as the power divider to equally split the input RF-power and the optimal microstrip 90º mitered bends used to reduce the loss. Each of the four sub-arrays has the same geometry structure as that of Array 1. The simulated results in Fig. 2 show that Array 3 achieves a wide impedance bandwidth of 57–66.2 GHz for $|S_{11}| < -10$ dB and a high peak gain of 14.98 dBi at 62.9 GHz, but the asymmetrical co-polarized radiation pattern in the E-plane and a high cross-polarization level in the H-plane as shown in Fig. 3(c) are similar to those of Array 1.

Based on the investigation of the advantages and disadvantages of Array 2 and Array 3, a 16-element parallel-series-fed patch antenna array with differential inputs is introduced as Array 4 in Fig. 1 d). The relative dimension values of each Array 3 in Array 4 are the same as those in Array 3 and the middle space labeled 1.2 mm is an optimized one. Due to the differential drive and eight compensated sub-arrays

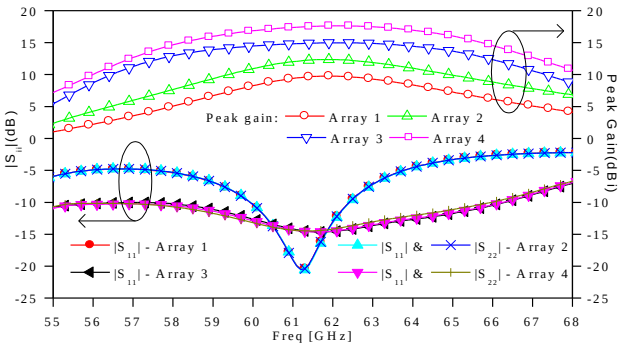

Fig. 2 Simulated reflection coefficients and peak gains of Array 1, Array 2, Array 3 and Array 4

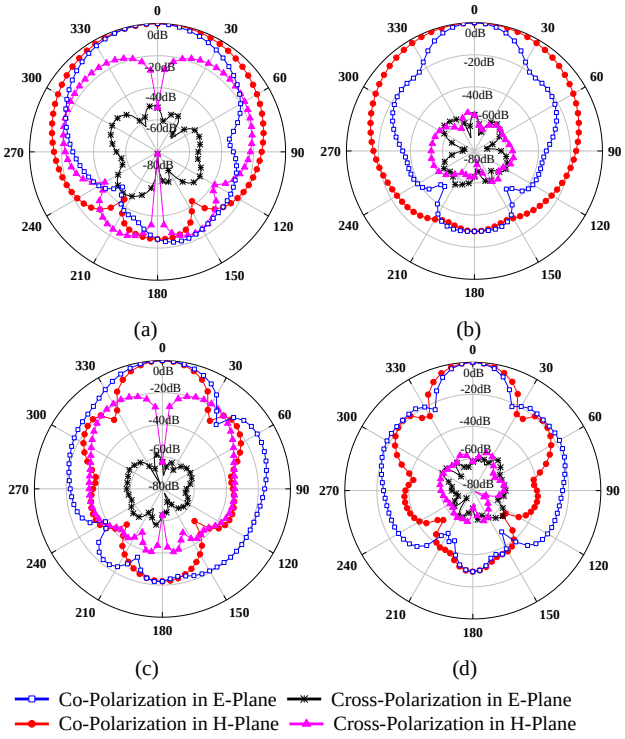

Fig. 3 Simulated radiation patterns of the designs in E- and H-planes @ 61.5 GHz for: (a) Array 1, (b) Array 2, (c) Array 3, (d) Array 4.

with connection in series and parallel, the simulated results in Fig. 2 and Fig. 3(d) show that Array 4 achieves significant improvement on the performance including the enhanced radiation patterns, wide impedance bandwidth and high peak gain of 17.62 dBi at 62.2 GHz. It is noteworthy that the proposed array has advantages of not only easy integration together with 60-GHz transceiver with differential-drive LNA or PA, but also better performance due to symmetrical and electrically balanced configuration.

When the receiver input or the transmitter output is single-ended port, the two-way power splitter with equal amplitude and 180 degree phase difference between the two output ports is introduced for the structure of Array 4 to convert from the single-ended drive port to the differential drive port as the structure given in Fig. 4. The quarter-wave matched T-junction and 90º mitered bends used in the two-way power splitter have the same dimensions as those of above mentioned one-to-four parallel-feed network. The required phase delay of the feed network is realized with the microstrip delay line. The final optimization is performed by tuning dimensions slightly

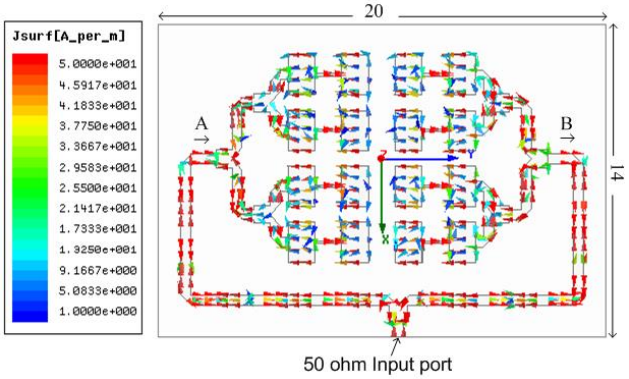

Fig. 4 Geometry of the proposed patch antenna array with simulated current distribution at 61.5 GHz (all dimensions expressed in millimeters).

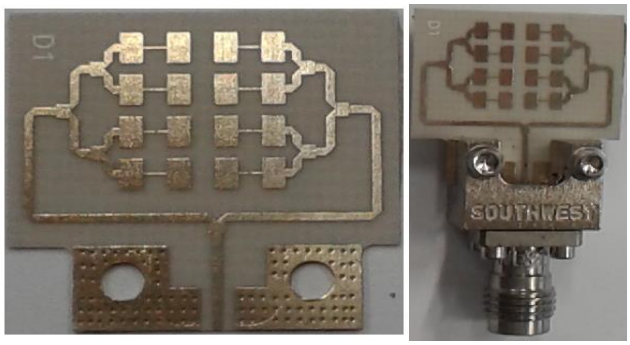

(a) (b)

Fig. 5 Photographs of the fabricated patch antenna array without and with the measurement connector.

with HFSS for improving the overall radiation characteristics and matching the input impedance of 50-ohm.

To illustrate the operation of the proposed antenna array, Fig. 4 shows the optimized 16-element patch antenna array with the current distribution of the radiating elements and feed network at 61.5 GHz in HFSS. It can be seen that the currents at the opposite points A and B are 180º out of phase with almost the same amplitude of current density so that the currents on all of the patch elements in phase result in radiation performance enhancement of the antenna array when the input port is excited.

For measuring the patch antenna array conveniently, the antenna-to-connector interface is designed for using the end launch connector which can provide low VSWR response up to 67 GHz [14]. The photographs of the fabricated patch antenna array without and with the end launch connector are shown in Fig. 5 (a) and (b) respectively. The size of the proposed patch antenna array is only 20 mm × 15 mm excluding the connector footprint for measurement.

III. MEASUREMENT RESULTS

The measurement was performed by using ROHDE& SCHWARZ ZVA67 vector network analyzer (VNA). In order to eliminate the effect of the end launch connector in the measured array gain, the insertion loss of the end launch connector was measured to be 1.21-1.86 dB with a back-to-back test configuration. The antenna measurement was implemented in a self-built environment by using the two identical patch antenna arrays which were placed with a separated distance R. During measurement, two identical

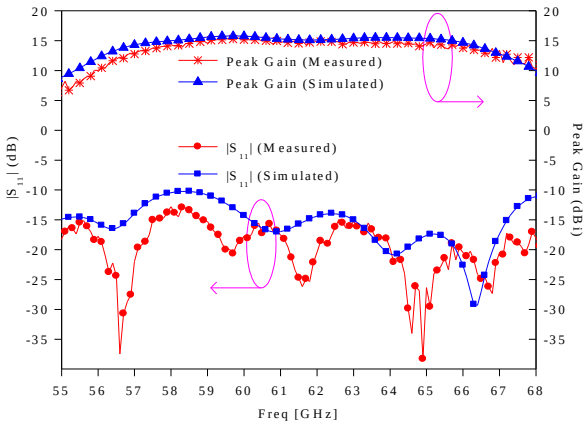

(a)

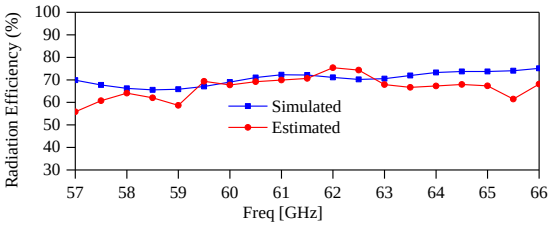

(b)

Fig. 6 Simulated and measured results of the proposed patch antenna array: (a) $|S_{11}|$ and Peak Gain, (b) radiation efficiencies.

patch antenna arrays were fixed face to face according to E-plane or H-plane and R should be satisfied with the far field condition in Equation (1).

$$R \geq \frac{2D^2}{\lambda} \quad (1)$$

Where D is the largest dimension of the patch antenna array and λ is the free space wavelength at the respective frequency. D = 20 mm is chosen for the measurement, hence it is enough to set the separated distance R equal to 610 mm during the measurement. From the Friis power transmission formula Equation (2), the gain of the tested antenna array was calculated by Equation (3).

$$P_{RX} = P_{TX} G_{RX} G_{TX} \frac{\lambda^2}{(4\pi R)^2} \quad (2)$$

$$G_T = \frac{1}{2}\left[20log_{10}\frac{4\pi R}{\lambda} + 10log_{10}\frac{P_{RX}}{P_{TX}}\right] \quad (3)$$

Where G_{Rx} and G_{Tx} are the gains of the receiving and transmitting antenna arrays, P_{Rx} and P_{Tx} are the powers received and transmitted respectively. Because the two antenna arrays are identical, G_{Rx} is the same as G_{Tx} and both are equal to the gain of the tested antenna array G_T ($G_{Rx} = G_{Tx} = G_T$). The power ratio of the received and transmitted powers (P_{Rx}/P_{Tx}) equals to the square of the voltage gain S_{12} or S_{21} which can be measured directly from the VNA.

Fig. 6 (a) shows the simulated and measured $|S_{11}|$ and the peak gain of the tested antenna array respectively. The good matching to 50-ohm is achieved with the $|S_{11}|$ less than -10 dB within the frequency range 55–68 GHz. The measured peak gain in Z-direction is 12.8-15.6 dBi between 57 and 66 GHz with the maximum peak gain of 15.52 dBi at 59.8 GHz. The measured gain agrees with the simulated gain.

To calculate the dielectric loss tangent of the substrate at 60

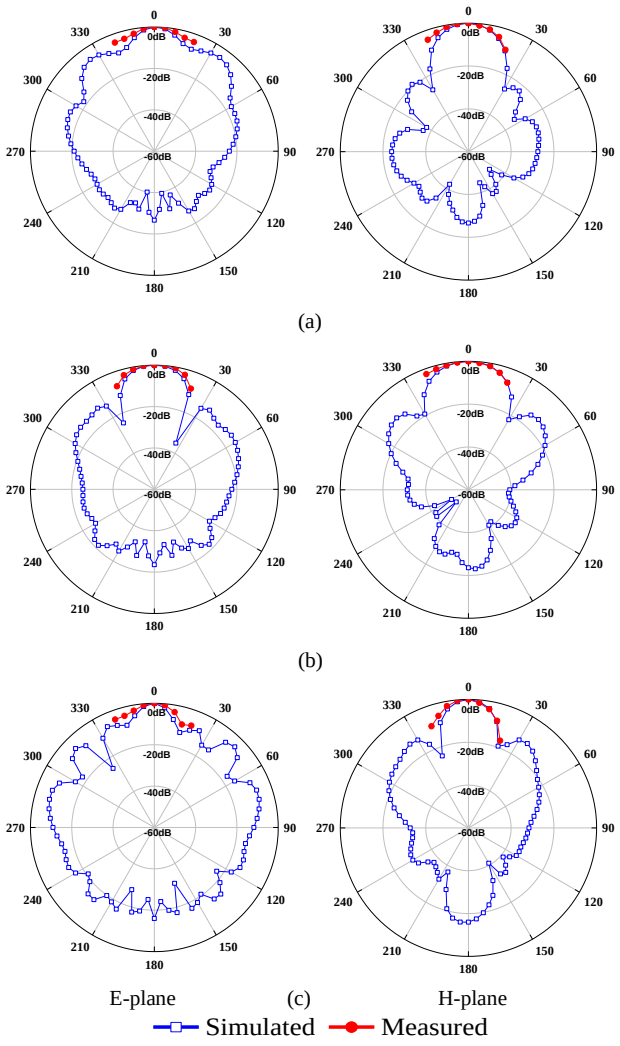

Fig. 7 Simulated and measured radiation patterns of the proposed patch antenna array in E-plane and H-plane (a) @ 57 GHz, (b) @ 61.5 GHz and (c) @ 66 GHz.

GHz, two microstrip lines with two different lengths (15 and 20 mm) were fabricated. The loss of a microstrip line with length = 5 mm is estimated by the subtraction between the measured transmission coefficients of the two microstrip lines. Then, the dielectric loss tangent at 60 GHz is extracted with tan δ = 0.0045 by comparing the estimated and simulated transmission coefficients of the microstrip line with length = 5 mm in HFSS. The radiation efficiency obtained from the measured gain and estimated directivity of the antenna array is about 67% at 60 GHz. The comparison between the simulated and estimated radiation efficiencies is shown in Fig. 6 (b).

Fig. 7 shows the normalized simulated and measured radiation patterns of the proposed patch antenna array at 57, 61.5 and 66 GHz. Due to the limitation of the measurement facility, the radiation patterns were measured only within ±20 degree from the broadside direction in the E- and H-plane respectively. The discrepancy between simulated and measured results is due to facility sensitivity and misalignment of the antennas, but the measured and simulated results still agree well with each other. Note that the sidelobe level becomes high in E-plane at 57 and 66 GHz respectively due to frequency dependency of the phase delay of the transmission lines, the feed network and patches together. To find sidelobe suppression techniques is the future study.

IV. CONCLUSION

In this letter, a low cost 60-GHz antenna array on a single substrate PCB is designed, fabricated and measured with a compact size. The gain and bandwidth benefits of hybrid using the parallel-series feed network together with the differential feeding technique are studied thoroughly and verified by experimental results. The designed antenna array achieves good performance with the measured $|S_{11}|$ of less than -10 dB within the frequency range 55–68 GHz and the measured peak gain of 12.8-15.6 dBi over the whole operating bandwidth from 57 to 66 GHz. The measured radiation patterns with –3 dB beamwidth at 61.5 GHz are around ±13º and ±15º in E- and H-plane respectively. With all of above features, the designed antenna array compatible with IEEE 802.11ad standard has high potential to be used in a 60-GHz wireless system.

REFERENCES

[1] A. E. I. Lamminen, J. Säily, and A. R. Vimpari, "60-GHz patch antennas and arrays on LTCC with embedded-cavity substrates," IEEE Trans. Antennas and Propagation, vol. 56, no. 9, pp. 2865–2874, Sep. 2008.

[2] S. Yeap, Z. N. Chen, and X. Qing, "Gain-enhanced 60-GHz LTCC antenna array with open air cavities," IEEE Trans. Antennas and Propagation, vol. 59, no. 9, pp. 3470–3473, Sep. 2011.

[3] J. F. Xu, Z.N.Chen, X. Qing, and W. Hong, "Bandwidth enhancement for a 60 GHz substrate integrated waveguide fed cavity array antenna on LTCC," IEEE Trans. Antennas and Propagation, vol. 59, no. 3, pp. 826-832, Mar. 2011.

[4] L. Wang, Y. X. Guo and W. X. Sheng, "Wideband High-Gain 60-GHz LTCC L-Probe Patch Antenna Array With a Soft Surface," IEEE Trans. Antennas and Propagation, Vol. 61, no.4, pp. 1802–1809, Apr. 2013.

[5] A. E. I. Lamminen, A. R. Vimpari, and J. Säily, "UC-EBG on LTCC for 60-GHz frequency band antenna applications," IEEE Trans. Antennas Propagation, vol. 57, no. 10, pp. 2904–2912, Oct. 2009.

[6] B. Zhang, D. Titz, F. Ferrero, C. Luxey, and Y. P. Zhang "Integration of quadruple linearly-polarized microstrip grid array antennas for 60-GHz antenna-in-package applications," IEEE Trans. Compon. Packag. Technol., vol. 3, pp. 1293-1300, Aug. 2013.

[7] H. Chu, Y. X. Guo and Z. L. Wang, "60-GHz LTCC Wideband Vertical Off-Center Dipole Antenna and Arrays," IEEE Trans. Antennas and Propagation, vol. 61, no. 1, pp. 153 - 161, Jan. 2013.

[8] Y. J. Li and K.-M. Luk, "A 60-GHz Dense Dielectric Patch Antenna Array," IEEE Trans. Antennas and Propagation, vol.62 no. 2, pp. 960 - 963, Feb. 2014.

[9] X. P. Chen, K. Wu, L. Han and F. F. He, "Low-Cost High Gain Planar Antenna Array for 60-GHz Band Applications," IEEE Trans. Antennas and Propagation, vol. 58, no. 6, pp. 2126 - 2129, June 2010.

[10] K. Gong, Z. N. Chen, X. Qing, P. Chen, and W. Hong, "Substrate integrated waveguide cavity-backed wide slot antenna for 60-GH bands," IEEE Trans. Antennas and Propagation, vol. 60, no. 12, pp. 6023 - 6026, Dec. 2012.

[11] Huang, J., "A parallel-series-fed microstrip array with high efficiency and low cross-polarization," Microwave and Optical Technology Letters, vol. 5, no. 5, pp. 230-233, May 1992.

[12] J. Säily, A. Lamminen, and J. Francey, "Low cost high gain antenna arrays for 60 GHz millimetre wave identification (MMID)," 2011. [Online]:http://www.taconic-add.com/pdf/technicalarticles--high_gain_antenna_mmid.pdf

[13] A. Bisognin, D. Titz, F. Ferrero, C. Luxey, G. Jacquemod, R. Pilard, F. Gianesello, D. Gloria and P. Brachat, "Differential feeding technique for mm-wave series-fed antenna-array," Electron. Lett., vol. 49 no. 15, pp. 918 - 919, 18th July 2013.

[14] http://mpd.southwestmicrowave.com/products/product.php?need=endLaunch&item=52.